Available online at www.sciencedirect.com
ScienceDirect
Trans. Nonferrous Met. Soc. China 29(2019) 1169−1183
Transactions of Nonferrous Metals Society of China
www.tnmsc.cn

Comparison of effect of SiC and MoS_2 on wear behavior of Al matrix composites

Mohammad ROUHI, Mohammad MOAZAMI-GOUDARZI, Mohammad ARDESTANI

Department of Materials Engineering, Science and Research Branch, Islamic Azad University, Tehran, Iran

Received 2 July 2018; accepted 19 December 2018

Abstract: In order to improve dry sliding wear resistance of pure aluminum against steel, aluminum-based composites reinforced with different contents of SiC, MoS_2 and SiC/MoS_2 particles were synthesized by press and sintering of the corresponding powder mixtures. The microstructural evaluations showed a dense microstructure which were in good agreement with the result of density and hardness measurements. The results of pin on disk wear tests performed against an AISI 52100 steel pin at a constant load and sliding velocity showed that there was a critical content for both types of the reinforcements at which the lowest wear rate was obtained, i.e. 10 vol.% and 2 vol.%, respectively, for Al/SiC and Al/MoS_2 composites. However, the lowest wear rate and friction of coefficient were attained for Al/10SiC/2MoS_2 hybrid composite. According to the scanning electron microscope observations, the predominant wear mechanism was changed from adhesion to abrasion mostly when MoS_2 particles were incorporated in the pure aluminum. Mild delamination was identified as the main wear mechanism for Al/SiC and Al/SiC/MoS_2 composites. The frictional traces and worn surfaces of Al/SiC/MoS_2 composites approached to those of Al/SiC composites, indicating the dominant role of SiC particles in tribological behavior of the hybrid composites.

Key words: Al/SiC/MoS_2 composites; microstructure; wear mechanism; friction

1 Introduction

Particle-reinforced metal matrix composites (PMMCs) have received much attention, due to their advantages toward monolithic alloys. Owing to low density and high heat conduction, aluminum is the most commonly used matrix material [1]. Reinforcement particles can be either harder or softer than the matrix phase. Aluminum matrix composites (AMCs) reinforced by hard particles (such as metal oxides and carbides) possess a higher specific strength and stiffness than that of the base metal. In addition, this type of AMCs exhibits improved hardness and wear resistance and low coefficient of thermal expansion [2]. On the other hand, soft particles (such as graphite and MoS_2) impart the metallic matrix with improved machinability [3] and anti-friction properties [4−6]. These properties provide a wide usage of AMCs in aeronautical [5], automotive [7,8] and thermal management [2,3] applications.

The wear rate of composite materials is usually influenced by both material and test parameters. Among material parameters, the volume fraction of reinforcing particles could be considered as the most important wear controlling parameter in both types of composites. Generally, the wear rate of PMMCs is reduced by increasing the volume fraction of either soft or hard particles provided that the interfacial bonding between the dispersed phase and matrix is strong enough [9]. However, some authors reported that the least wear rate was attained when an optimized amount of hard particles was used [10]. A similar observation has been reported for composites reinforced by soft lubricant particles [11]. On the other hand, the result of some investigations showed that by increasing the volume fraction of soft particles, both abrasive [12] and sliding [13] wear rates were increased. These contradictory results may arise from different processing procedures or testing conditions.

Composites that contain more than one type of reinforcing particles are called hybrid composites [14]. One of the remarkable types of hybrid composites is the metal matrix composites (MMCs) reinforced by both soft and hard particles. It is expected that a hybrid composite

Corresponding author: Mohammad MOAZAMI-GOUDARZI; Tel: +98-21-44869783; E-mail: moazami@srbiau.ac.ir
DOI: 10.1016/S1003-6326(19)65025-9

benefits from the properties of both soft and hard particles. For instance, it was found out that the wear rate of Al6061/SiC/Gr hybrid composites was lower than that of Al6061/SiC and Al6061/Gr composites [15−17]. RAVINDRAN et al [18] reported the increased coefficient of friction and wear resistance due to the addition of hard SiC particles to Al2024/5wt.%Gr composites. ZEREN [19] reported that addition of up to 6 wt.% graphite to Al/SiC composite resulted in reduction of hardness and volume loss. MOSLEH-SHIRAZI et al [20] achieved the minimum wear rate in Al/SiC nanocomposites by adding 2 vol.% graphite to the composite. The beneficial effect of soft MoS_2 particles on improved wear resistance of Al/Al_2O_3 composites was also reported by other researchers [21,22]. The formation of a protective layer between contacting surfaces is the main reason for reducing the wear rate in hybrid composites. The increased wear resistance of aluminum alloys by formation of a hybrid composite layer through processes such as friction stir processing was also reported [23,24].

A literature review shows that most investigations have only studied the effect of one type of reinforcing particles on wear resistance of the hybrid MMCs. The purpose of this work is to study the tribological behavior of Al/SiC, Al/MoS_2 and Al/SiC/MoS_2 composites. The effect of volume fraction of each reinforcing particles on the wear mechanism is discussed. The focus has been on differences in tribological features of AMCs contained different types of reinforcements.

2 Experimental

Pure Al, SiC and MoS_2 powders with mass median diameters of 32, 57 and 17 μm, respectively, were used as starting materials. Figure 1 shows the SEM images of these powder particles together with their corresponding size characteristics. The size distribution of powders was obtained by a CILAS 1064 laser particle size analyzer. In order to produce AMCs containing 5, 10 and 20 vol.% SiC, and 2, 4 and 6 vol.% MoS_2, predetermined amounts of each powder were weighed according to Table 1 and then blended in a roller mixer. Powder mixtures were pressed in a steel cylindrical mold with an inner diameter of 25 mm under a constant pressure of 700 MPa. Subsequently, the produced green compacts were sintered in a tube type furnace at 620 °C for 1 h in N_2 atmosphere. X-ray diffraction (XRD) was performed on the sintered compacts using a Philips PW−1730 diffractometer with Cu K_α radiation.

Densities of sintered specimens were determined by Archimedes' principle. Microstructural studies were performed on polished surfaces of the specimens by OLYMPUS BX51M optical microscope. Hardness of the specimens was measured with an ESEWAY Vickers hardness tester under a load of 294 N.

Wear tests were performed on rotating disk specimens using a pin on disk tribometer device, according to ASTM G99-95a standard in an atmosphere with 30%−40% humidity at 25 °C. AISI 52100 bearing steel pins with 3 mm in diameter and 40 mm in height were used as the counterfaces. The hardness of the pins

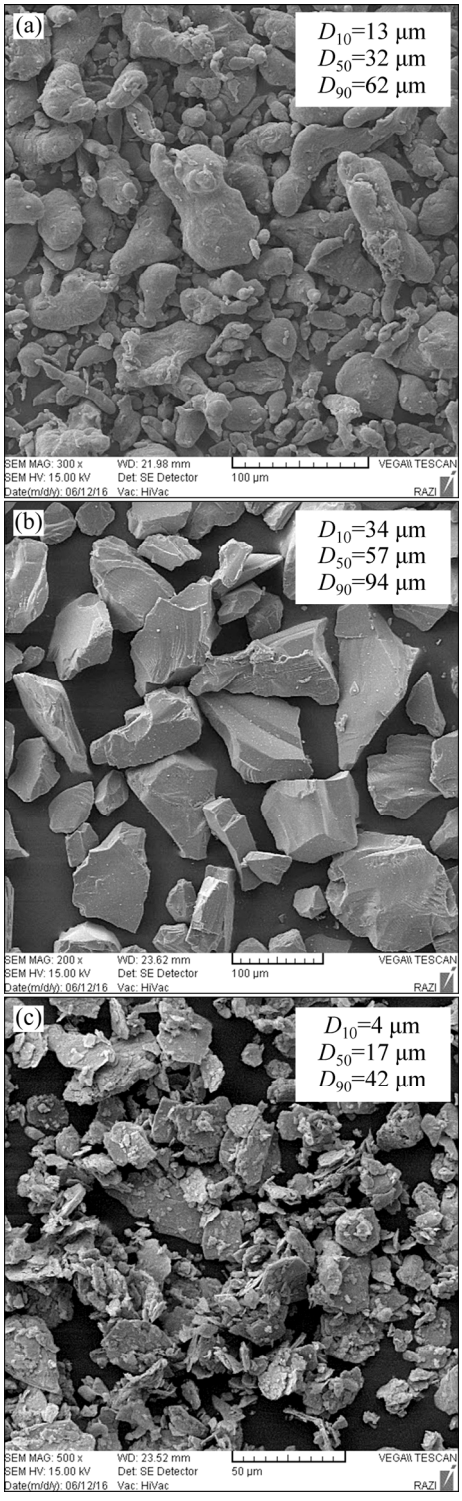

Fig. 1 SEM micrographs of as-received Al (a), SiC (b) and MoS_2 (c) powders

Table 1 Volume fractions of Al, MoS_2 and SiC powders in prepared powder mixtures

No.	Volume fraction/%		
	Al	SiC	MoS_2
1	100	–	–
2	95	5	–
3	90	10	–
4	80	20	–
5	98	–	2
6	96	–	4
7	94	–	6
8	88	10	2
9	86	10	4
10	84	10	6

was HRC 62. Before each test, the specimens and pins were cleaned in acetone using an ultrasonic device. The force applied to pins was 5 N and the rotational speed of disk was 0.1 m/s. The mass loss of the steel pins and specimens was measured using an analytical balance with the accuracy of 0.1 mg after a sliding distance of 1000 m. The wear surfaces and debris were studied by a VEGA TESCAN scanning electron microscope equipped with an energy-dispersive X-ray spectroscopy (EDS) analyzer. In addition, the worn aluminum and composite test disks were sectioned across their longitudinal axis in order to study the subsurface regions.

3 Results and discussion

3.1 Microstructure, density and hardness

Figure 2 shows the optical microscopy images from the cross section of the sintered aluminum and Al/SiC composites. As observed in Fig. 2(a), no boundary can be detected between aluminum powder particles and a nearly dense microstructure is produced. This microstructure indicates that the applied sintering condition is appropriate for producing a consolidated aluminum powder product.

Figures 2(b−d) show that individual SiC particles are distributed within the aluminum matrix and minor agglomeration is observed. Homogenous distribution is the most important microstructural characteristic of PMMCs [25]. Furthermore, primary boundaries of the powder particles in Al/SiC composite specimens are not observed. This shows that the sintering process was performed well and resulted in consolidation of the composite compacts. Dark regions observed in the microstructure of Al/SiC composites may represent either ordinary porosities not been eliminated by sintering or voids left behind by detachment of SiC particles in the polishing stage of sample preparation. It is clear from Fig. 2 that the amount of porosities in the microstructure was increased by increasing volume fraction of SiC particles.

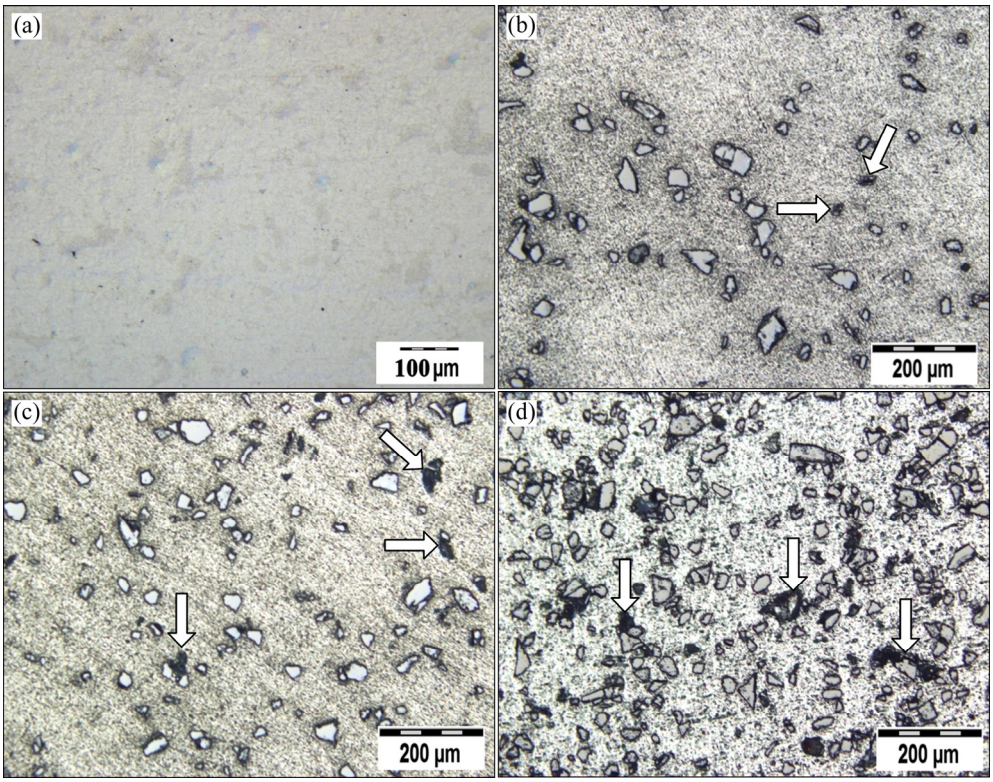

Fig. 2 Microstructures of pure Al (a) and Al/5SiC (b), Al/10SiC (c) and Al/20SiC (d) composites (Some porosities are marked with arrows)

The microstructures of Al/2MoS_2, Al/6MoS_2, Al/10SiC/2MoS_2 and Al/10SiC/6MoS_2 composites are shown in Figs. 3(a−d), respectively. These microstructures reveal that distribution of both MoS_2 and SiC particles within the aluminum matrix is reasonably uniform. However, some agglomerated MoS_2 particles are also observed within the microstructure, which is due to the adhesive nature of this constituent. It seems that by increasing the volume fraction of the reinforcements, the volume fraction of microstructural porosities was increased.

The result of XRD analysis performed on Al/6MoS_2 composite, as a representative, is shown in Fig. 4. As observed, the obtained pattern shows only Al and MoS_2 peaks indicating stability of MoS_2 at the applied sintering condition.

Figure 5(a) shows the effect of SiC content on the hardness and relative density of Al/SiC composites. It was found that the relative density of sintered compacts decreased with increasing volume fraction of SiC particles. The melting temperature of SiC particles is much higher than that of aluminum. Therefore, these ceramic particles were not sintered at the utilized sintering temperature (620 °C). In addition, SiC particles retard sintering of aluminum powders by locating between them and acting as a diffusion barrier. In addition, the increase in the number of agglomerates for composites with a higher volume of reinforcing particles could be another reason for reduction of relative density with increasing SiC content. It is further clear from Fig. 5(a) that the hardness of Al/SiC composites showed a peak at 5 vol.% SiC addition above which the hardness gradually decreased. SiC is a hard constituent and it is anticipated that the hardness of the composites increases with increasing SiC content. However, the reduced relative sintered density of the composites containing higher SiC contents resulted in reduction of hardness.

Figure 5(b) shows the effect of MoS_2 content on the relative density and hardness of Al/MoS_2 and Al/10SiC/MoS_2 composites. It is evident that both the relative density and hardness decreased with increasing MoS_2 content, regardless of the content of SiC particles. Similar results were reported by other researchers on the influence of MoS_2 particles on the hardness and relative density of MMCs. XIONG [26] reported that increasing the amount of MoS_2 up to 6 vol.% decreased the hardness and relative density of the composite material. The hardness of SiC is higher than that of the aluminum matrix. In addition, the coefficient of thermal expansion of SiC differs from that of aluminum. As a result, an increase in hardness of the material is expected when SiC particles are incorporated within the aluminum matrix [27]. However, MoS_2 is a soft phase and unlike SiC does not increase density of dislocations within aluminum matrix. In addition, according to Fig. 5(b), MoS_2 particles adversely affected the relative sintered density of powder compacts which in turn resulted in further reduction in hardness of composite materials.

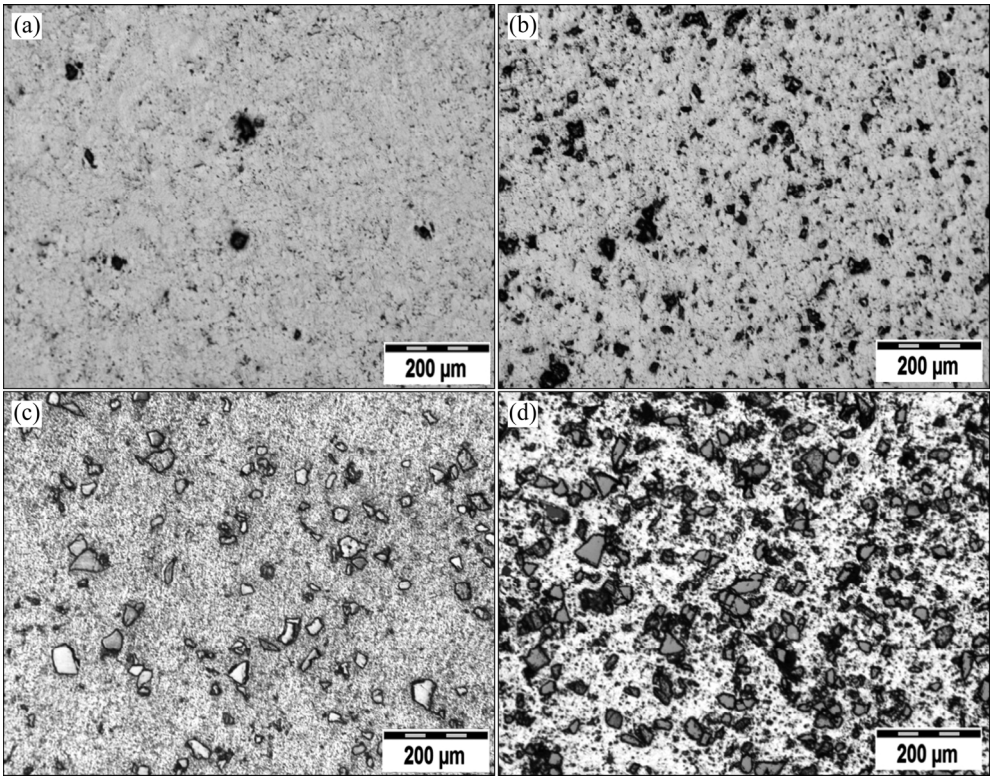

Fig. 3 Microstructures of Al/2MoS_2 (a), Al/6MoS_2 (b), Al/10SiC/2MoS_2 (c) and Al/10SiC/6MoS_2 (d) composites

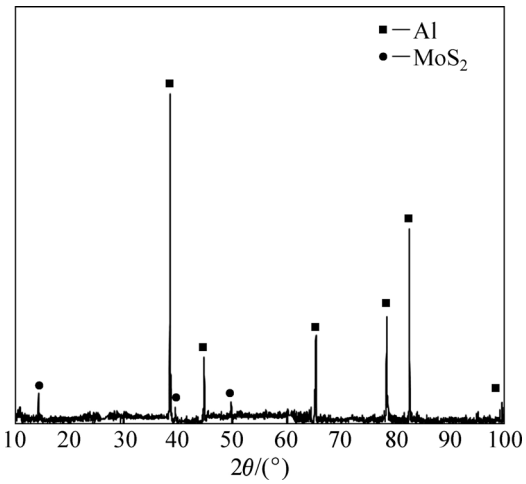

Fig. 4 XRD pattern of sintered Al/6MOS_2 composite

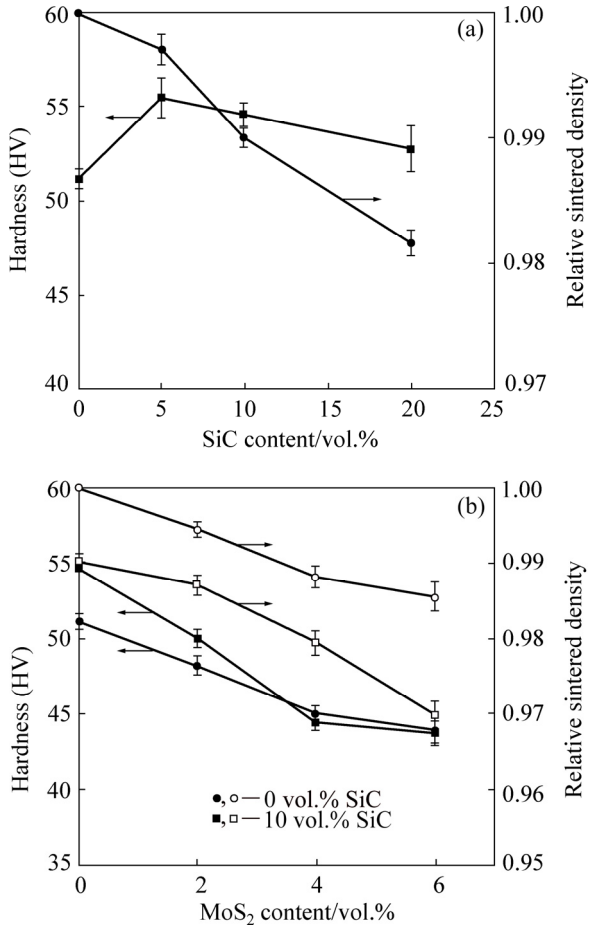

Fig. 5 Variation of hardness and relative sintered density with SiC content in Al/SiC composites (a) and MoS_2 content in Al/MoS_2 and Al/10SiC/MoS_2 composites (b)

3.2 Wear rate

Figure 6(a) shows the variation of wear rate of Al/SiC composites with SiC content. It was observed that the volume loss of Al/SiC composites was far less than that of unreinforced aluminum. The wear rate was

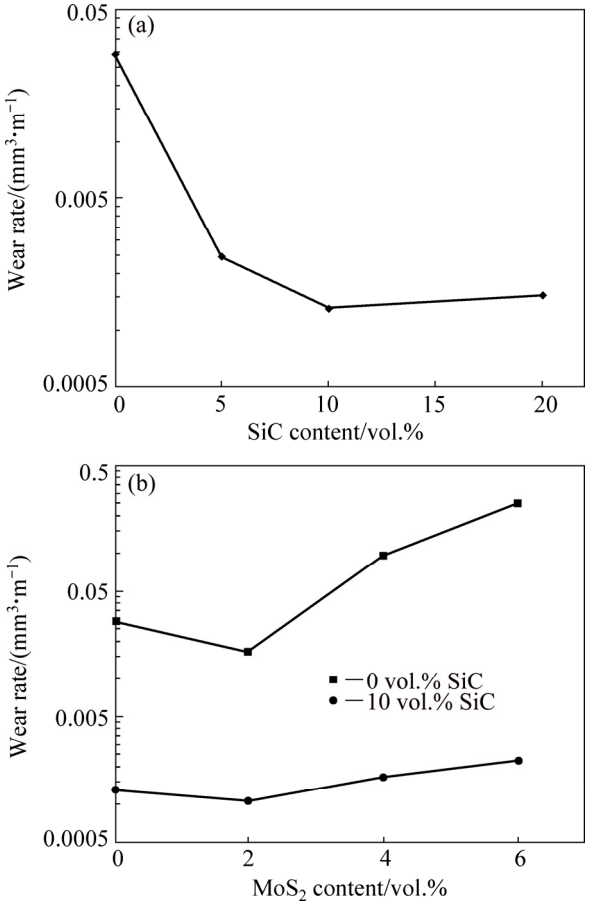

Fig. 6 Variation of wear rate of Al/SiC composites with SiC content (a) and Al/MoS_2 and Al/10SiC/MoS_2 composites with MoS_2 content (b)

considerably reduced by addition of 5 vol.% SiC. The wear rate of Al/10SiC composite was 50% lower than that of Al/5SiC composite, while, according to Fig. 5(a), hardness of the latter was marginally higher. The wear rate was slightly increased by increasing SiC content from 10 vol.% to 20 vol.%. This was mainly due to the higher hardness of Al/10SiC composite (Fig. 5(a)). According to the Archard equation [28], the wear volume of materials is inversely proportional to their hardness. Furthermore, the relative sintered density decreased when SiC content increased from 10 vol.% to 20 vol.% (Fig. 5(a)). This indicates that Al/20SiC composite contains higher microstructural porosities deteriorating its toughness. The wear resistance of materials is decreased by either increased porosity or decreased toughness [29]. Therefore, the lower wear resistance of Al/20SiC composite as compared to that of Al/10SiC could be attributed to the lower hardness and relative density of the former. The existence of an optimum content of hard ceramic particles to achieve the least wear rate in AMCs has also been reported by other authors [16,30].

Figure 6(b) shows variation of wear rates of

Al/MoS_2 and Al/10SiC/MoS_2 composites with MoS_2 content. It was found that, the wear rate was decreased by increasing MoS_2 content from 0 to 2 vol.%, regardless of the SiC content. This is because of the lubricating effect of MoS_2 particles. However, when MoS_2 content exceeded this threshold, the wear rate increased so that the wear rate of Al/4MoS_2 composite was higher than that of pure aluminum. The reason for this is that both hardness and relative density were considerably decreased by increasing MoS_2 content (Fig. 5(b)). High wear losses in MMCs containing high content of MoS_2 particles were also reported [31]. In addition, Fig. 6(b) reveals that hybrid Al/10SiC/MoS_2 composites were more resistant to wear than Al/MoS_2 composites. The minimum wear rate was attained for Al/10SiC/2MoS_2 composite. The wear rate of this composite was even 25% lower than that of Al/10SiC composite. In fact, utilizing the optimized contents of both types of reinforcements resulted in achieving the highest wear resistance for Al/10SiC/2MoS_2 hybrid composite.

Figure 7 shows the variation of wear rate of the counterface (steel pin). As shown in Fig. 7(a), wear rate of the pin counterface increased with increasing content of SiC particles in the rotating disk. The steel pin in contact with the unreinforced aluminum showed mass gain. This can be caused by mass transfer from the aluminum disk to the steel pin. The mass transfer in sliding wear occurs by formation and then breakage of adhesive bonds at the asperities of the mating surfaces. However, the content of SiC particles in the disk samples resulted in mass loss of the steel pins during sliding. The abrasive action of SiC particles on the pin surface was intensified by increasing SiC content. Figure 7(b) shows variation of wear rate of the counterfaces in contact with Al/MoS_2 and Al/10SiC/MoS_2 composite disk. The wear rate of the counterface in contact with Al/MoS_2 composite was not considerably changed by increasing the MoS_2 content. However, in the counterfaces in contact with the hybrid specimens, the wear rate slightly increased with increasing MoS_2 content of the disk.

In summary, the results of the wear test showed that addition of either soft MoS_2 or hard SiC reinforcing particles increased the wear resistance of aluminum provided that their content was limited to a critical value. A comparison between the effect of SiC and MoS_2 on enhancing the wear resistance of pure aluminum indicates the superior impact of hard SiC particles (Fig. 6). Addition of 10 vol.% SiC decreased the wear rate of aluminum by 90%. While, in the best circumstances, addition of 2 vol.% of MoS_2 to aluminum was accompanied with a 42% reduction in the wear rate. The profound effect of SiC particles on reduction of wear rate could be ascribed to the higher hardness and relative density of Al/10SiC composite in comparison to that of

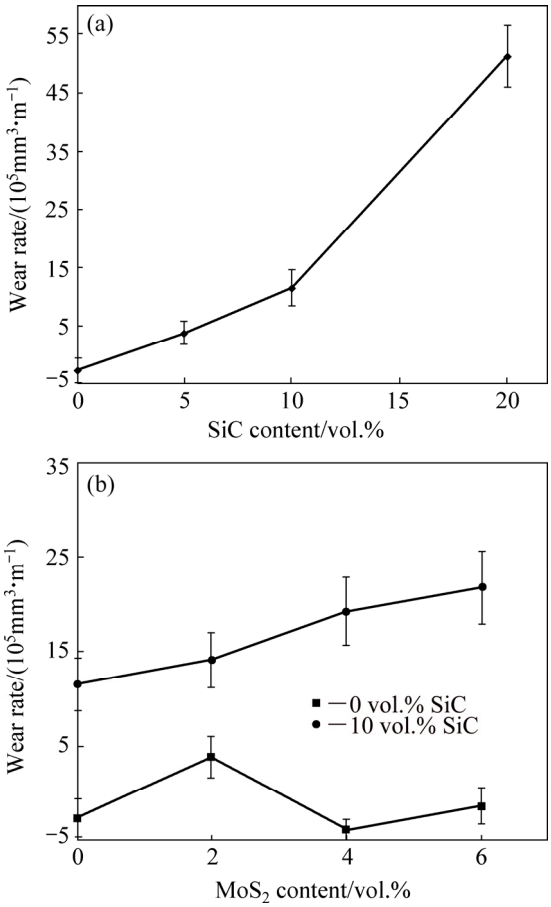

Fig. 7 Variation of wear rate of counterface (steel pin) with SiC content of Al/SiC composites (a) and with MoS_2 content of Al/MoS_2 and Al/10SiC/MoS_2 composites (b)

the Al/2MoS_2 composite. However, the reduction of wear rate in the Al/SiC composite specimens was accompanied by increasing the wear rate of the counter steel pin (Fig. 7). In fact, superior hardness and wear resistance of the Al/SiC composites deteriorated the wear resistance of the tribosystems through increasing the wear rate of the counterface. Whereas, the wear rate of counterface did not change considerably by addition of soft MoS_2 particles to the aluminum matrix disks. As a result, the best tribological performance was attained by using the Al/10SiC/2MoS_2 hybrid composite. While the wear rate of this hybrid composite was 97% lower than that of unreinforced aluminum, no severe abrasion was observed for the mating counterface.

3.3 Wear mechanism

Figure 8 shows SEM images of the wear surface and debris together with result of EDS analysis for the pure aluminum disk. The worn surface of pure aluminum sample (Fig. 8(a)) was subjected to severe plastic deformation with large protrusions indicating excessive adhesive wear. The results of EDS analysis show the

absence of aluminum oxide layer on the worn surface. As observed in Fig. 8(b), the generated debris particles have irregular shapes and are very large (>100 μm). These irregularly shaped chunky particles are usually caused by adhesive wear [32]. The formation of large wear debris resulted in inferior wear resistance of pure aluminum disk (Fig. 6). According to EDS analysis, these particles comprise of mostly aluminum and are poor in oxygen implying the absence of oxidative wear.

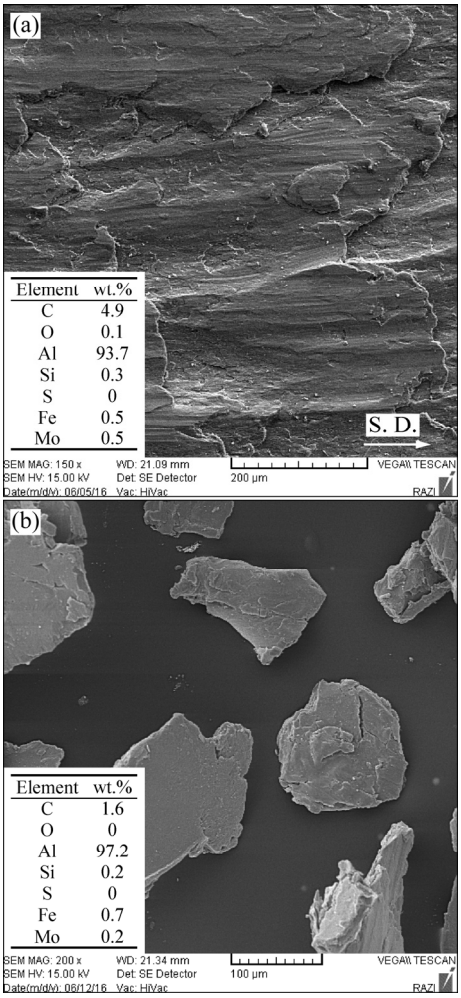

Fig. 8 SEM micrographs of wear surface of pure Al (a) and generated debris (b) together with their corresponding EDS analysis results (The arrow shows the sliding direction)

Figure 9 presents the SEM images of wear surfaces of Al/SiC composites together with their EDS analysis results. As evident from Fig. 9(a), the extent of plastic deformation on worn surface of Al/5SiC composite is much lower than that of unreinforced aluminum (Fig. 8(a)). In addition, some cracks and platelets are observed on the wear surface of Al/5SiC composite. The existence of these platelets that their front edges oppose the sliding direction could be a sign of delamination [33]. The worn surface of Al/10SiC shown in Fig. 9(b) relatively resembles to that of Al/5SiC composite. Some parts of

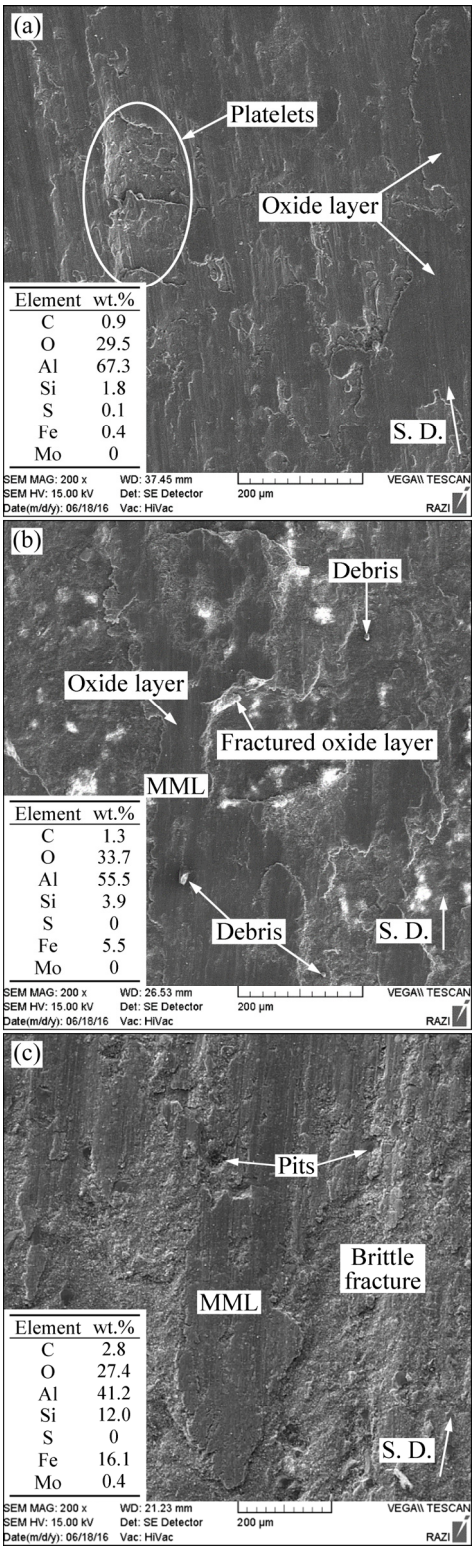

Fig. 9 SEM micrographs of wear surface of Al/5SiC (a), Al/10SiC (b) and Al/20SiC (c) composites (The arrows show the sliding direction)

the worn surface are completely smooth and some others show slight plastic deformation. The EDS analysis results indicate that smooth areas are rich in oxygen and iron as well as aluminum. This suggests the mass transfer

from the steel counterface and its oxidization. In fact, during the sliding, hard SiC particles within the composite disk abrade the steel pin. Subsequently, the worn particles are severely deformed and oxidized forming a mechanically mixed layer (MML). This tribolayer is hard and protects the surface of the composite material from further wear damage resulting in reduction of the wear rate [29,34]. The white marks on the worn surface may indicate the fractured oxide layers as confirmed by EDS analysis. These results clearly indicate that the oxidative wear mechanism was active during the sliding of Al/SiC composites against the steel counterface. The plastically deformed areas on the surface of Al/10SiC composite represent minor adhesive wear. Furthermore, Fig. 9(b) shows that some of the worn particles are embedded on the surface of composite disk under the applied force existed between the surfaces in contact. This also decreased the wear rate of the Al/10SiC composite. The worn surface of Al/20SiC composite, as shown in Fig. 9(c), is also covered by the MML in some smooth areas. However, some surface detachments which are caused by brittle fracture mechanism are also observed. This mechanism was activated because the relative density of Al/20SiC composite was inferior to that of Al/5SiC and Al/10SiC composites. Similar to Al/10SiC composite, the worn surface of Al/20SiC was rich in oxygen and iron confirming the formation of the MML in some regions. However, it seems that the amount of reinforcement particles in Al/5SiC composite was not sufficient for creation of MML as its worn surface was poor in iron. The lower wear rates obtained for Al/10SiC and Al/20SiC composites as compared to that of Al/5SiC with a higher hardness could be attributed to the protective role of MML formed on their surfaces.

Figure 10 shows the SEM images of wear particles of Al/SiC composites together with their EDS analysis results. The generated debris particles show two different morphologies. The smaller particles have a powder-like form and the larger particles are thin platelets. In addition, the size of the wear particles decreased with increasing SiC content of the composite. As the volume fraction of SiC particle increased, the contact of these ceramic particles with the steel counterface increased. This causes higher abrasion of the pin material that may lead to three-body wear forming smaller debris. The morphology of small wear particles is similar to that generated in another investigation at low applied loads [35]. Those large but thin flake debris particles were generated due to the delamination wear mechanism. Generally, delaminated materials are large flake-like particles. However, the plowing action of the counterface can break these particles and form particles in different shapes [36].

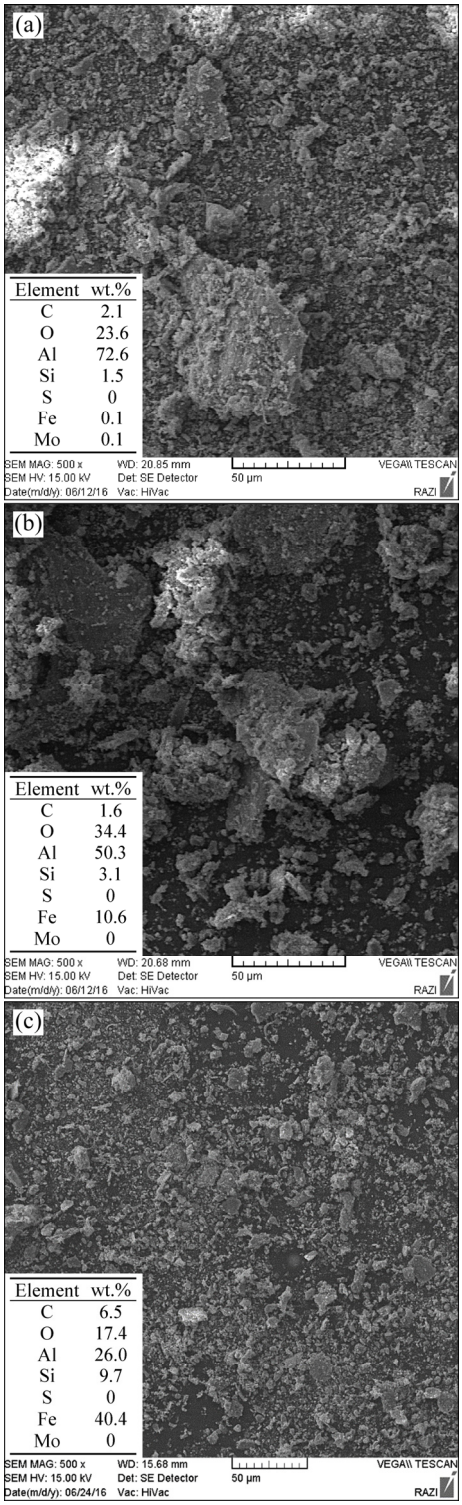

Fig. 10 SEM micrographs of generated wear debris of Al/5SiC (a), Al/10SiC (b) and Al/20SiC (c) composites

According to EDS results presented in Fig. 10, the wear debris of Al/SiC disks contained relatively high oxygen content. This indicates that the generated wear particles of Al/SiC composites are predominantly oxide unlike that of unreinforced aluminum which is mainly metallic (Fig. 8(b)). It seems that the oxidation of the generated wear particles has been induced due to their

fineness. The existence of the oxidized fine worn debris implies mild wear process [37]. Figures 10(b−c) show that the wear debris of the composites containing 10 vol.% and especially 20 vol.% SiC particles composed of significant amount of iron. As discussed earlier, this is due to the abrasive action of SiC particles on the steel counterface.

Figure 11 presents the SEM images of wear surface of the Al/MoS_2 composite disks together with their EDS analysis results. The wear surface of Al/2MoS_2 composite, as shown in Fig. 11(a), is covered by parallel grooves in the slip direction indicating the two-body abrasive wear. As known, the wear rate of two-body abrasive wear is usually higher than that of the three-body wear [38]. Therefore, a higher wear rate was attained for this specimen as compared to that of Al/10SiC composite (Fig. 6). In addition, it seems that the white lines on the worn surface of Al/2MoS_2 composite represent the broken oxidized layer. The EDS analysis of this specimen indicates the existence of an oxide layer as well as a film rich in sulfur and molybdenum (the MoS_2 lubricant layer) on the surface. During the wear test, the MoS_2 particles come out to the surface of the composite under the applied load. These particles are then smeared on the surface of composite disk in a way that the areas in contact are covered by a lubricant layer of MoS_2. This lubricant film decreases metal to metal contact on the mating surfaces. As a result, the wear rate is reduced as compared with that of the pure aluminum (Fig. 6(b)).

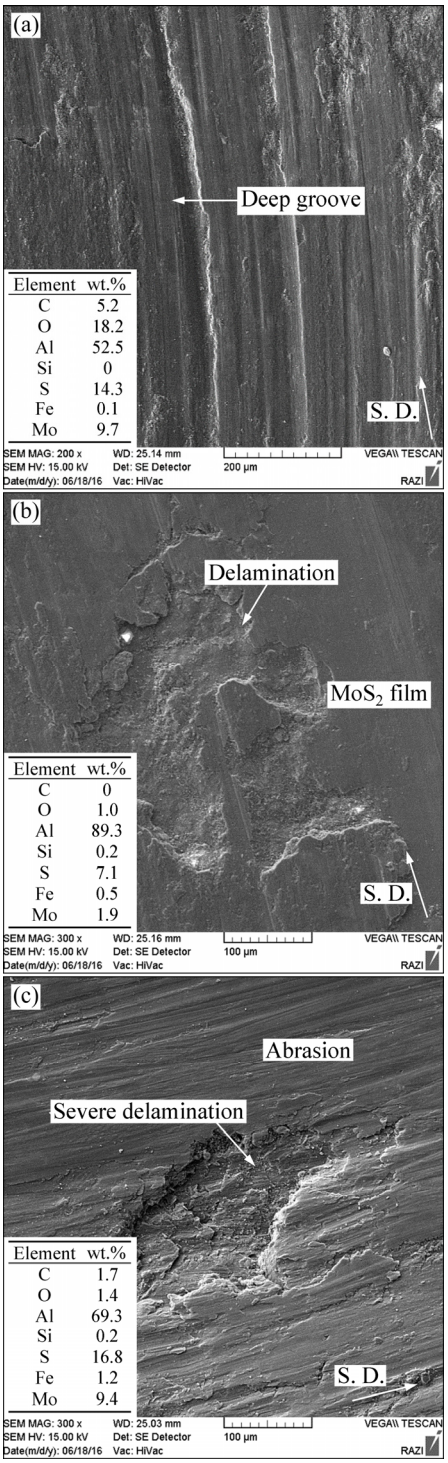

Fig. 11 SEM micrographs of wear surface of Al/2MoS_2 (a), Al/4MoS_2 (b) and Al/6MoS_2 (c) composites (The arrows show the sliding direction)

The worn surface of the Al/4MoS_2 composite is shown in Fig. 11(b). It was found that increasing the MoS_2 content from 2 vol.% to 4 vol.% resulted in reduction of abrasive wear and increasing of delamination wear. In addition, formation of a smooth and dark film of MoS_2 lubricant layer is evident on the worn surface. This decreased the oxygen content on the wear surface of Al/4MoS_2 composite. On the wear surface of the specimens containing 6 vol.% MoS_2 (Fig. 11(c)), sever delamination as well as abrasion marks are observed. Based on the hardness values reported in Fig. 5, the hardness of both Al/4MoS_2 and Al/6MoS_2 samples was low. Therefore, in these composite disks, the created lubricant layer may not adhere firmly to the surface and could be easily detached under shear stresses applied by the counterface during sliding. This would activate the delamination wear mechanism and deteriorate the wear resistance of the materials. As shown in Fig. 6(b), the wear rates of the composites containing 4 vol.% and 6 vol.% MoS_2 particles were even more than that of the unreinforced aluminum. The effectiveness of a solid lubricant material in reducing the metal to metal contact during sliding depends on the ability of the sheared lubricant layers in adhering to the sliding surface [13]. It seems that when the MoS_2 content exceeded 2 vol.% the adhesion force between the lubricant layer and the material surface became lower than shear strength of MoS_2 particles. As a consequence, the MoS_2 lubricant layer did not effectively adhere to the materials surface and was easily delaminated.

Figure 12 shows the SEM images of wear debris of the Al/MoS_2 composites. Regardless of the volume

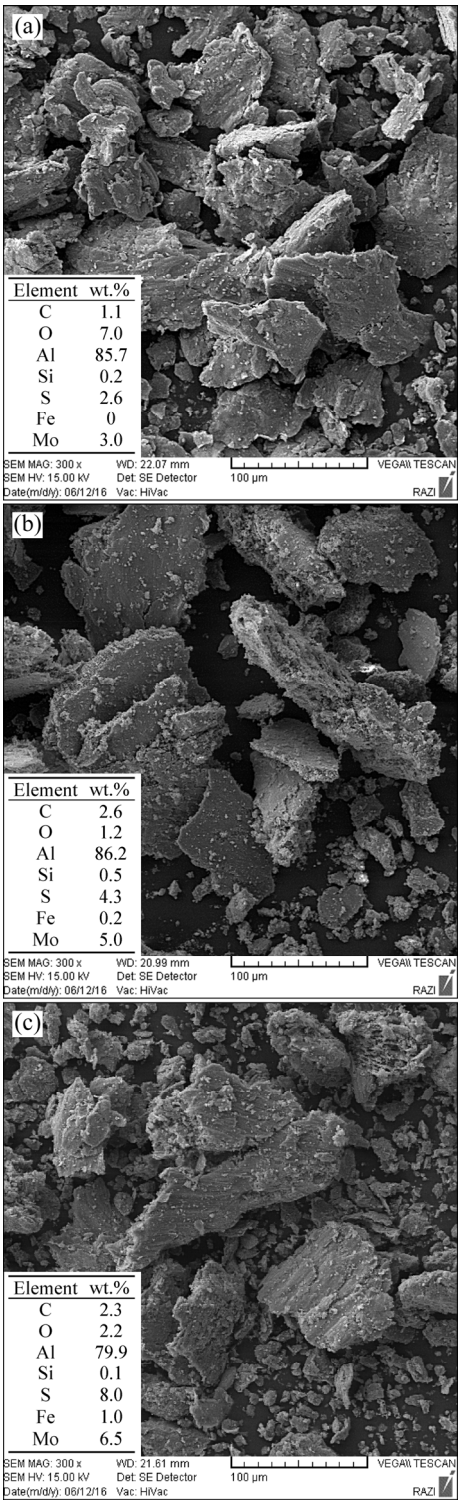

Fig. 12 SEM micrographs of generated wear debris of Al/2MoS_2 (a), Al/4MoS_2 (b) and Al/6MoS_2 (c) composites

fraction of MoS_2 particles, the wear particles were mostly large (~100 μm) and sheet-like. However, some smaller debris particles (~10 μm) are also observed. The wear sheets of Al/MoS_2 disks are even thicker than those of unreinforced aluminum (Fig. 8(b)). This is because of the lower hardness and frictional stress on the wear surface of Al/MoS_2 composites [39]. While the morphology of the wear particles did not depend on MoS_2 volume fraction, their thickness slightly increased as MoS_2 content increased from 2 vol.% to 6 vol.%. In addition, the fraction of the smaller wear particles increased with increasing MoS_2 content. This could be attributed to the reduced relative density and increased structural discontinuities in the aluminum matrix due to the existence of higher content of MoS_2 particles in the composite. In the case of Al/6MoS_2 composite, the shape of wear particles (Fig. 12(c)) approaches to the typical shape of debris generating by abrasive wear of brittle materials [9]. It was also found that the generated wear debris of Al/MoS_2 composites was larger than that of Al/SiC composites (Fig. 10) resulting in higher wear rate for the Al/MoS_2 composites. In addition, the wear debris of Al/MoS_2 composites was relatively poor in oxygen that further discriminates them from that of Al/SiC composites.

The worn surface of Al/10SiC/2MoS_2 hybrid composite, as shown in Fig. 13(a), was mainly composed of parallel superficial scratches indicating mild abrasion. In addition, the plastic deformation and the fracture of oxidized layer are also observed. The EDS analysis results confirmed the formation of MML on the wear surface. The existence of lower contents of Mo and S on the wear surface as compared to those of O and Fe shows that the tribological behavior of Al/10SiC/2MoS_2 hybrid composites was mostly controlled by the oxidized MML formed on the surface of the material. In other words, the role of the hard SiC particles in tribological behavior of the hybrid composites was more effective than that of soft lubricant MoS_2 particles. Consequently, it is anticipated that the wear surface and debris features of Al/10SiC/2MoS_2 hybrid composite approach to those of Al/10SiC composite. The wear debris of the Al/10SiC/2MoS_2 hybrid composite, as observed in Fig. 13(b), consists of fine equiaxed particles and small sheets. The morphology of these particles is similar to that of Al/SiC composites. However, the wear debris is smaller in the hybrid composite. In fact, by addition of MoS_2 particles to Al/10SiC composite, the structural discontinuity in the aluminum matrix increases, resulting in generation of smaller debris. As a result, the minimum wear rate was obtained for the Al/10SiC/2MoS_2 hybrid composite. Like Al/10SiC composite, the wear debris of the hybrid composite contained a significant amount of iron and oxygen, indicating micro-cutting of steel pin and generation of iron/iron oxide debris.

3.4 Subsurface deformation

Figure 14 shows the SEM images of the section under the wear surface for aluminum and the composites. Figure 14(a) reveals an intense deformation of the material just beneath the worn surface for the Al disk.

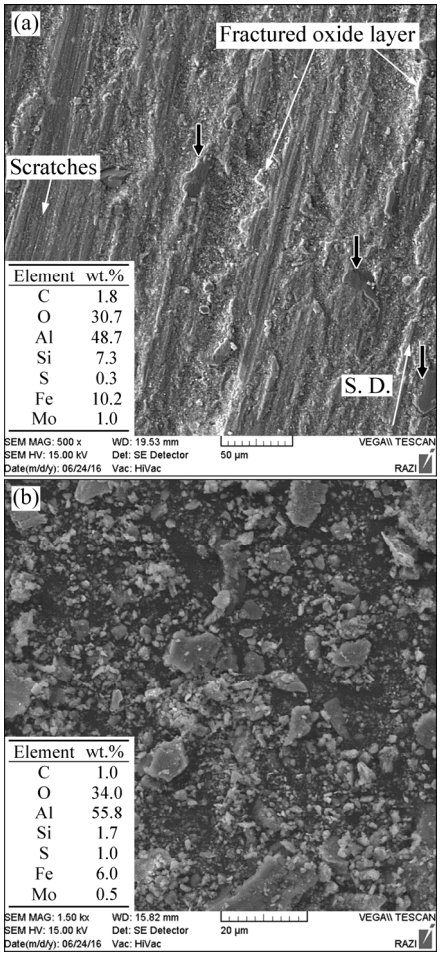

Fig. 13 SEM micrographs of wear surface of Al/10SiC/2MoS_2 hybrid composite (a) and generated debris (b) (Black short arrows show some protruding SiC particles)

This is due to the frictional shear force applied by the counterface. Therefore, as observed, a lamellar structure was developed directly below the worn surface due to intense strain induced by sliding. As the distance from the worn surface increases, the induced strain decreases and hence grains maintain their original shape. Finally, an inhomogeneous deformation zone developed in subsurface regions. However, there is no sign of subsurface cracks for pure aluminum specimen. This indicates that formation of the wear particles in unreinforced aluminum is due to the asperity rupture and its adhesive transfer to the counterface. Because of this adhesive transfer the mass of counterface was increased in the wear test (Fig. 7(a)).

In cross-sectional microstructure of the worn Al/10SiC composite (Fig. 14(b)) a protruding SiC particle is seen. This type of reinforcements is in contact with the counterface and concentrates the wear damage on the steel pin. However, the inhomogeneous shear deformation of the subsurface regions resulted in interfacial decohesion and crack initiation at the reinforcing particles. During the wear process, dislocations accumulate in surface regions. In these circumstances, different mechanisms are suggested for formation of cavities and cracks. The slip of moving dislocations, produced by the applied normal force, is usually restricted by the hard reinforcing particles. Therefore, the rate of crack initiation in a metal matrix is increased by the existence of hard particles. Since the strength of SiC particles is higher than cohesive strength of the aluminum matrix, the cracks nucleate due to the stress induced by dislocations pile-up. Cavities are usually generated by decohesion along the interface of the matrix and particles during the plastic deformation. In particular, the inhomogeneous plastic flow of the matrix around the hard particles could result in cavity formation. In addition, the formation of cracks around the hard particles is considered as the most important mechanism for cavity formation. However, the formation of cracks and cavities under the surface is not necessarily accompanied by the formation of wear particles. Wear particles are only formed when the cracks and cavities coalescence in a way that strength of subsurface layer becomes lower than the applied shear stress established between the material and counterface. The crack propagation, cavities growth and shear plastic deformation of the metal between the cavities are the three main mechanisms for joining of cracks and cavities [39]. The crack propagation and interfacial decohesion mechanisms for Al/10SiC composite are evident in Fig. 14(b). In agreement with the well-documented delamination theory of wear [40], the cracks nucleated at the interface between reinforcements (SiC particles) and aluminum matrix and then propagated parallel to surface. The same mechanism was found for formation of wear debris in Al/2MoS_2 composites as shown in Fig. 14(c). Furthermore, since the strength of reinforcing MoS_2 particles is too low, the stress caused by dislocation pile-up breaks these soft particles and forms cavities in them. However, it seems that because of the low hardness of Al/MoS_2 composites as compared to that of Al/SiC composites (Fig. 5), more plastic constraint is applied to surface of Al/MoS_2 composites by the counterface. Therefore, in the case of Al/MoS_2 composites, cracks inevitably nucleated and propagated at relatively deep layers of subsurface region. As a result, thicker wear particles were formed. The wear debris of Al/10SiC/2MoS_2 hybrid composite was mostly generated by interfacial decohesion and crack propagation mechanisms as shown in Fig. 14(d).

3.5 Coefficient of friction

Figure 15(a) shows the variation of average coefficient of friction as a function of SiC content for Al/SiC composites. The coefficient of friction decreased

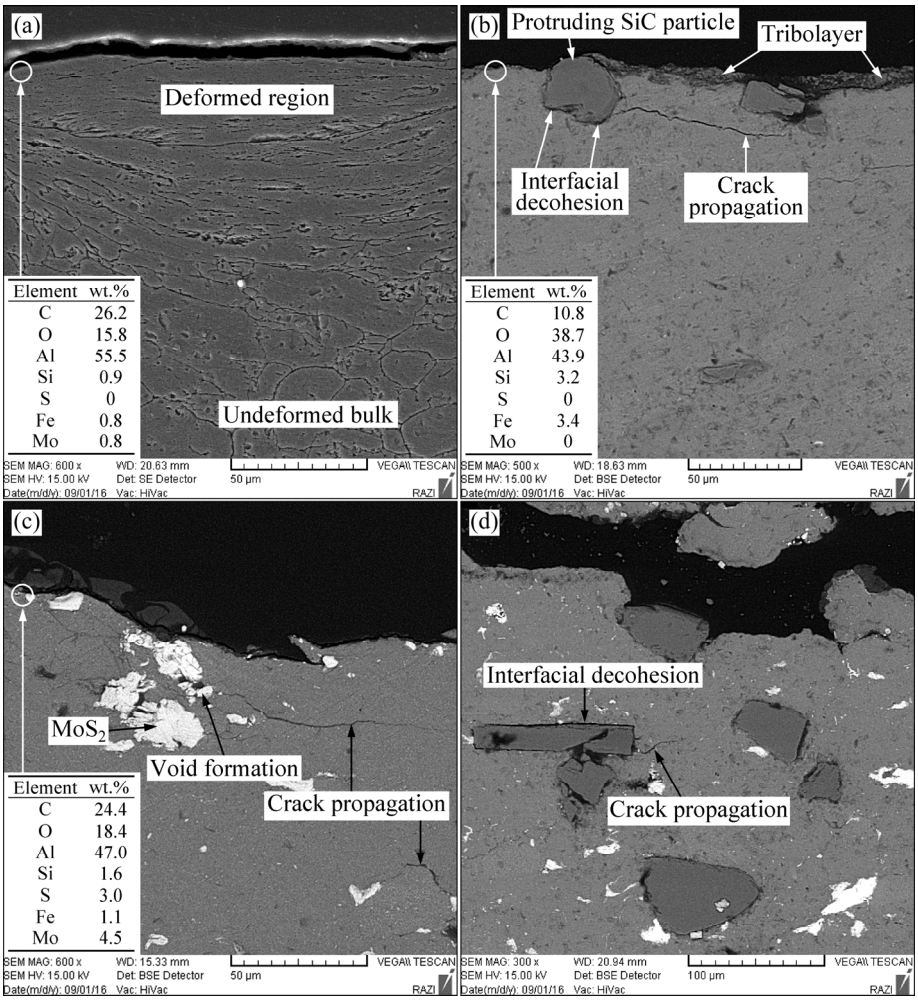

Fig. 14 SEM micrographs of transverse cross-sections of subsurface for pure Al (a), Al/10SiC composite (b), Al/2MoS_2 composite (c) and Al/10SiC/2MoS_2 hybrid composite (d)

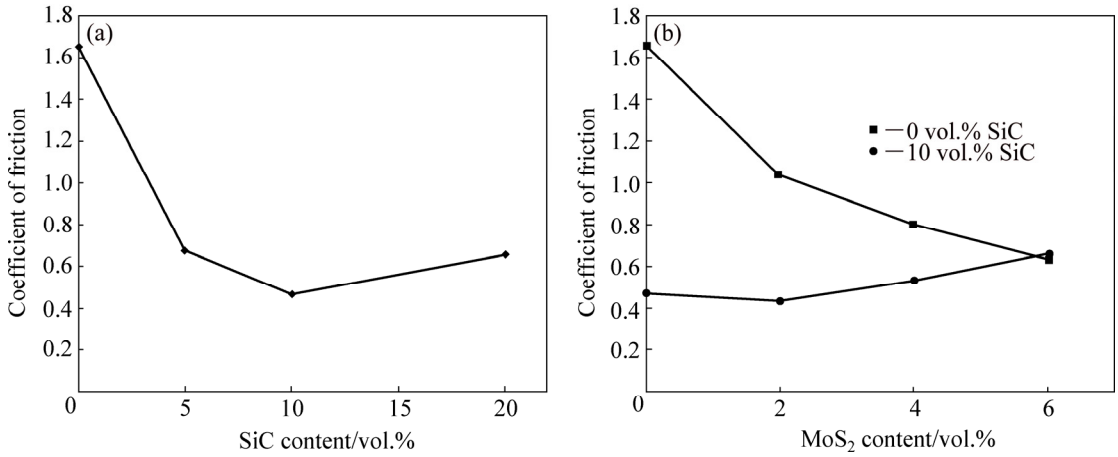

Fig. 15 Variation of coefficient of friction of Al/SiC composites with SiC content (a) and Al/MoS_2 and Al/10SiC/MoS_2 composites with MoS_2 content (b)

with increasing SiC content up to 10 vol.%. This is due to the lubricating role of MML formed on the wear surface [41]. However, the coefficient of friction increased when SiC content increased from 10 vol.% to 20 vol.%. This could be attributed to the increased plastic deformation on the wear surface of Al/20SiC composite (Fig. 9(c)) due to its reduced hardness (Fig. 5(a)). In addition, the higher volume porosity of Al/20SiC composite encouraged the crack coalescence. This resulted in detachment of MML through debris

generation. As a result, the coefficient of friction increased. The overall trend of variation of coefficient of friction with SiC content is identical to that of wear rate presented in Fig. 6(a). This implies the importance of coefficient of friction in controlling the wear volume of the material. In the case of Al/MoS_2 composites, the average coefficient of friction decreased with increasing MoS_2 content as shown in Fig. 15(b). However, the least coefficient of friction was attained for the Al/10SiC/2MoS_2 composite.

In addition to the average coefficient of friction, its variation with wear distance during the sliding can also provide useful information about the tribological behavior of the material. Figure 16 shows the friction traces for pure aluminum and its composites. Dissimilar frictional characteristics are evident for different materials. The coefficient of friction for pure aluminum disk, as presented in Fig. 16(a), is unstable with violent fluctuations throughout the sliding distance. This kind of friction variation with sliding distance is categorized as severe fluctuation type [42]. The friction trace of Al/10SiC composite (Fig. 16(b)) exhibits a relatively steady coefficient of friction after a very short running-in distance. This stable trend could be attributed to the lubricating role of the MML layer formed on the wear surface. The friction trace of Al/2MoS_2 composite (Fig. 16(c)) starts with a severely fluctuated running-in period which continues for about 200 m. During this time period, MoS_2 particles are squeezed out from the matrix and smeared on the wearing surfaces. Consequently, both coefficient of friction and its fluctuation decrease and the friction trace reaches a nearly stable stage. The most stable friction trace was obtained for Al/10SiC/2MoS_2 composite under the lubricating effect of both MML and MoS_2 film.

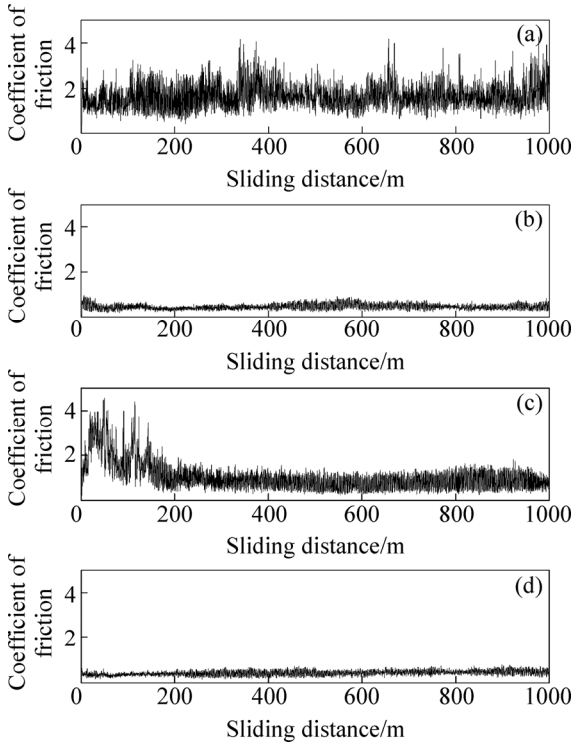

Fig. 16 Friction traces for pure Al (a), Al/10SiC composite (b), Al/2MoS_2 composite (c) and Al/10SiC/2MoS_2 hybrid composite (d)

4 Conclusions

(1) The microstructural characterization showed that the distribution of both types of reinforcements within the aluminum matrix was reasonably uniform. Increasing the volume fraction of the reinforcing particles was followed by the reduction of relative density. However, the highest hardness was obtained for Al/5SiC composite.

(2) Addition of 10 vol.% SiC and 2 vol.% MoS_2 to aluminum decreased the wear rate by 90% and 42%, respectively. The composites containing more than 2 vol.% MoS_2 particles showed higher wear rate than that of unreinforced aluminum. The improved wear resistance of the composites containing SiC particles was attributed to formation of a protective MML on the wear surface.

(3) The least coefficient of friction and wear rate were obtained for Al/10SiC/2MoS_2 hybrid composite. Excellent feature of the hybrid composites was manifested in considerable reduction in the wear rate of the steel counterface.

(4) Adhesion was found as the dominant wear mechanism for the unreinforced aluminum. In the case of Al/SiC composites, however, mild delamination was the dominant wear mechanism. Abrasion as well as heavy delamination wear mechanisms predominated for Al/MoS_2 composites.

(5) Wear debris were generated by adhesive transfer mechanism in unreinforced aluminum. However, subsurface crack propagation parallel to the worn surface was the main mechanism for formation of wear particles in the composite disks. Interfacial decohesion also encouraged this process in Al/SiC composites. In the case of Al/MoS_2 composites, formation of subsurface cavities contributed to the debris generation.

(6) The friction traces of pure aluminum fluctuated severely. Formation of a solid lubricating MoS_2 film on the wear surface of Al/2MoS_2 composite decreased the friction fluctuations. However, the composites containing SiC particles exhibited a more stable friction.

(7) The friction characteristics and wear surfaces of the Al/SiC/MoS_2 hybrid composites were similar to those of Al/SiC composites, indicating the important influence of hard SiC particles on controlling tribological behavior of the hybrid composites.

References

[1] IBRAHIM I A, MOHAMED F A, LAVERNIA E J. Particulate reinforced metal matrix composites—A review [J]. Journal of Materials Science, 1991, 26: 1137−1156.

[2] MIRACLE D. Metal matrix composites — From science to technological significance [J]. Composites Science and Technology, 2005, 65: 2526-2540.

[3] LLOYD D J. Particle reinforced aluminium and magnesium matrix composites [J]. International Materials Reviews, 1994, 39: 1-23.

[4] RAMESH C S, NOOR AHMED R, MUJEEBU M A, ABDULLAH M Z. Development and performance analysis of novel cast copper−SiC−Gr hybrid composites [J]. Materials & Design, 2009, 30: 1957−1965.

[5] RAWAL S P. Metal-matrix composites for space applications [J]. JOM Journal of the Minerals Metals and Materials Society, 2001, 53: 14−17.

[6] MOAZAMI-GOUDARZI M, NEMATI A. Tribological behavior of self lubricating Cu/MoS_2 composites fabricated by powder metallurgy [J]. Transactions of Nonferrous Metals Society of China, 2018, 28: 946−956.

[7] PRASAD S V, ASTHANA R. Aluminum metal-matrix composites for automotive applications: tribological considerations [J]. Tribology letters, 2004, 17: 445−453.

[8] ROHATGI P. Cast aluminum-matrix composites for automotive applications [J]. JOM Journal of the Minerals Metals and Materials Society, 1991, 43: 10−15.

[9] Friction, lubrication, and wear technology [M]. Vol. 18. USA: ASM International, 1992.

[10] ANAND K., KISHORE. On the wear of aluminium-corundum composites [J]. Wear, 1983, 85: 163−169.

[11] DHANASEKARAN S, GNANAMOORTHY R. Dry sliding friction and wear characteristics of Fe−C−Cu alloy containing molybdenum di sulphide [J]. Materials & Design, 2007, 28: 1135−1141.

[12] KOVALCHENKO A M, FUSHCHICH O I, DANYLUK S. The tribological properties and mechanism of wear of Cu-based sintered powder materials containing molybdenum disulfide and molybdenum diselenite under unlubricated sliding against copper [J]. Wear, 2012, 290−291: 106−123.

[13] JHA A K, PRASAD S V, UPADHYAYA G S. Sintered 6061 aluminium alloy−solid lubricant particle composites: Sliding wear and mechanisms of lubrication [J]. Wear, 1989, 133: 163−172.

[14] CHAWLA N, CHAWLA K K. Metal matrix composites: Cyclic fatigue [M]. New York: Springer, 2013: 227−282.

[15] MAHDAVI S, AKHLAGHI F. Effect of the graphite content on the tribological behavior of Al/Gr and Al/30SiC/Gr composites processed by in situ powder metallurgy (IPM) method [J]. Tribology Letters, 2011, 44: 1−12.

[16] MAHDAVI S, AKHLAGHI F. Effect of SiC content on the processing, compaction behavior, and properties of Al6061/SiC/Gr hybrid composites [J]. Journal of Materials Science, 2011, 46: 1502−1511.

[17] MAHDAVI S, AKHLAGHI F. Effect of the SiC particle size on the dry sliding wear behavior of SiC and SiC−Gr-reinforced Al6061 composites [J]. Journal of Materials Science, 2011, 46: 7883−7894.

[18] RAVINDRAN P, MANISEKAR K, RATHIKA P, NARAYANASAMY P. Tribological properties of powder metallurgy−Processed aluminium self lubricating hybrid composites with SiC additions [J]. Materials & Design, 2013, 45: 561−570.

[19] ZEREN A. Effect of the graphite content on the tribological properties of hybrid Al/SiC/Gr composites processed by powder metallurgy [J]. Industrial Lubrication and Tribology, 2015, 67: 262−268.

[20] MOSLEH-SHIRAZI S, AKHLAGHI F, LI D Y. Effect of graphite content on the wear behavior of Al/2SiC/Gr hybrid nano-composites respectively in the ambient environment and an acidic solution [J]. Tribology International, 2016, 103: 620−628.

[21] KANTHAVEL K, SUMESH K R, SARAVANAKUMAR P. Study of tribological properties on Al/Al_2O_3/MoS_2 hybrid composite processed by powder metallurgy [J]. Alexandria Engineering Journal, 2016, 55: 13−17.

[22] KUMAR M, MISHRA A K. Mechanical behavior of Al 6063/MoS_2/Al_2O_3 hybrid metal matrix composites [J]. International Journal of Scientific and Research Publications, 2014, 4: 1−4.

[23] ALIDOKHT S A, ABDOLLAH-ZADEH A, ASSADI H. Effect of applied load on the dry sliding wear behaviour and the subsurface deformation on hybrid metal matrix composite [J]. Wear, 2013, 305: 291−298.

[24] SOLEYMANI S, ABDOLLAH-ZADEH A, ALIDOKHT S A. Microstructural and tribological properties of Al5083 based surface hybrid composite produced by friction stir processing [J]. Wear, 2012, 278−279: 41−47.

[25] TAHA M A. Practicalization of cast metal matrix composites (MMCCs) [J]. Materials & Design, 2001, 22: 431−441.

[26] XIONG Dang-sheng. Lubrication behavior of Ni−Cr-based alloys containing MoS_2 at high temperature [J]. Wear, 2001, 251: 1094−1099.

[27] SEKINE H, CHENT R. A combined microstructure strengthening analysis of SiC_p/Al metal matrix composites [J]. Composites, 1995, 26: 183−188.

[28] ARCHARD J F. Contact and rubbing of flat surfaces [J]. Journal of Applied Physics, 1953, 24: 981−988.

[29] MOAZAMI-GOUDARZI M, AKHLAGHI F. Wear behavior of Al 5252 alloy reinforced with micrometric and nanometric SiC particles [J]. Tribology International, 2016, 102: 28−37.

[30] ERDEMIR F, CANAKCI A, VAROL T, OZKAYA S. Corrosion and wear behavior of functionally graded Al2024/SiC composites produced by hot pressing and consolidation [J]. Journal of Alloys and Compounds, 2015, 644: 589−596.

[31] NARAYANASAMY P, SELVAKUMAR N, BALASUNDAR P. Effect of hybridizing MoS_2 on the tribological behaviour of Mg−TiC composites [J]. Transactions of the Indian Institute of Metals, 2015, 68: 911−925.

[32] STACHOWIAK G W, BATCHELOR A W, STACHOWIAK G B. Tribology Series: Wear particle analysis [M]. GWIDON W. STACHOWIAK A W B, GRAZYNA B S, ed. Elsevier, 2004: 253−294.

[33] JAHANMIR S. The relationship of tangential stress to wear particle formation mechanisms [J]. Wear, 1985, 103: 233−252.

[34] VENKATARAMAN B, SUNDARARAJAN G. The sliding wear behaviour of Al-SiC particulate composites—II. The characterization of subsurface deformation and correlation with wear behaviour [J]. Acta Materialia, 1996, 44: 461−473.

[35] LI X Y, TANDON K N. Microstructural characterization of mechanically mixed layer and wear debris in sliding wear of an Al alloy and an Al based composite [J]. Wear, 2000, 245: 148−161.

[36] ZHAN Yong-zhong, ZHANG Guo-ding. Friction and wear behavior of copper matrix composites reinforced with SiC and graphite particles [J]. Tribology letters, 2004, 17: 91−98.

[37] MENEZES P, NOSONOVSKY M, INGOLE S P, KAILAS S V, LOVELL M R. Tribology for scientists and engineers: From basics to advanced concepts [M]. 1st ed. New York: Springer, 2013.

[38] HUTCHINGS I M. Tribology: Friction and wear of engineering materials [M]. 1st ed. London: Edward Arnold, 1992.

[39] SUH Nam P. The delamination theory of wear [J]. Wear, 1973, 25: 111−124.
[40] SUH Nam P. An overview of the delamination theory of wear [J]. Wear, 1977, 44: 1−16.
[41] LI X Y, TANDON K N. Mechanical mixing induced by sliding wear of an Al−Si alloy against M2 steel [J]. Wear, 1999, 225−229, Part 1: 640−648.
[42] MA Wen-lin, LU Jin-jun. Effect of sliding speed on surface modification and tribological behavior of copper–graphite composite [J]. Tribology Letters, 2011, 41: 363−370.

比较研究 SiC 和 MoS_2 对铝基复合材料磨损行为影响

Mohammad ROUHI, Mohammad MOAZAMI-GOUDARZI, Mohammad ARDESTANI

Department of Materials Engineering, Science and Research Branch, Islamic Azad University, Tehran, Iran

摘　要：为了提高纯铝对钢的干滑动摩擦耐磨性，通过压制烧结混合粉末的方法制备不同 SiC、MoS_2 和 SiC/MoS_2 颗粒含量的铝基复合材料。显微结构分析表明，该合金结构致密，这与密度和硬度测试结果相吻合。在恒定载荷和滑动速度下进行复合材料与对偶为 AISI 52100 钢的销-盘式磨损试验。结果显示，当 Al/SiC 和 Al/MoS_2 复合材料中增强相的最佳含量分别为 10 vol%和 2 vol%时，材料的磨损率最低；而 Al/10SiC/2MoS_2 复合材料的磨损率和摩擦因数最低。扫描电镜观察表明，在纯铝中加入 MoS_2 颗粒后，材料的主要磨损机理由粘着磨损转变为以磨粒磨损为主。对于 Al/SiC 和 Al/SiC/MoS_2 复合材料，其主要的磨损机理为轻微的剥层磨损。Al/SiC/MoS_2 复合材料与 Al/SiC 复合材料的摩痕和磨损表面接近，表明 SiC 颗粒在这两种复合材料摩擦学行为中起主导作用。

关键词：Al/SiC/MoS_2 复合材料；显微结构；磨损机制；摩擦

(Edited by Xiang-qun LI)